

# The effects of operating conditions on the performance of a direct carbon fuel cell

ANDRZEJ KACPRZAK  
RAFAŁ KOBYLECKI\*  
ZBIGNIEW BIS

Czestochowa University of Technology, Department of Energy Engineering,  
Brzeźnicka 60a, 42-200 Częstochowa, Poland

**Abstract** The influences of various operating conditions including cathode inlet air flow rate, electrolyte temperature and fuel particles size on the performance of the direct carbon fuel cell DCFC were presented and discussed in this paper. The experimental results indicated that the cell performance was enhanced with increases of the cathode inlet gas flow rate and cell temperature. Binary alkali hydroxide mixture (NaOH-LiOH, 90–10 mol%) was used as electrolyte and the biochar of apple tree origin carbonized at 873 K was used as fuel. Low melting temperature of the electrolyte and its good ionic conductivity enabled to operate the DCFC at medium temperatures of 723–773 K. The highest current density ( $601 \text{ A m}^{-2}$ ) was obtained for temperature 773 K and air flow rate  $8.3 \times 10^6 \text{ m}^3\text{s}^{-1}$ . It was shown that too low or too high air flow rates negatively affect the cell performance. The results also indicated that the operation of the DCFC could be improved by proper selection of the fuel particle size.

**Keywords:** Direct carbon fuel cell; Biochar; Molten hydroxide electrolyte; Carbon anode; Air cathode

## 1 Introduction

The direct carbon fuel cell (DCFC) is a power generation device converting the chemical energy of carbon directly into electricity by electrochemical oxidation of the fuel [1]. The basic structure of a direct carbon fuel cell

---

\*Corresponding Author. E-mail: rafalk@is.pcz.czest.pl.pl

is identical to any of the other fuel cells. Each cell consists of a cathode and anode separated by electronically insulating but ionically conducting electrolyte. The only difference is that the anode chamber is supplied with a solid carbonaceous fuel (e.g., hard coals, biomass-derived biochars, active carbons, carbon black, graphite, coke, etc.) that is oxidized directly at the electrode surface. The DCFC technology is relatively simple compared to other fuel cell technologies and requires no expensive preparation of any gaseous fuel, as well as accepts all carbonaceous substances, as potential fuels. The theoretical maximum efficiency of carbon conversion in the DCFC is 100% [1] but practical efficiencies have been demonstrated at roughly 80% [2].

So far, three different electrolyte concepts have been proposed for the DCFC technology: molten hydroxide, molten carbonate or solid oxygen ion conducting ceramic [3]. The direct carbon fuel cell with molten hydroxide electrolyte is considered as to be the most promising type of DCFCs, due to its advantages [4], such as high ionic conductivity and high electrochemical activity of the carbon. Accordingly, the DCFC may be operated at lower temperatures (roughly 673–873 K) and thus cheaper materials may be used to manufacture the cell. Despite those advantages, the technology is still at an early stage of development and requires further research focused on investigation of the reaction kinetics, fuel delivery, materials degradation and optimal operation parameters, before this technology will come to the phase of commercialization.

This paper, presents in detail the various operating conditions (electrolyte temperature, cathode air flow rate, fuel particles size) on the performance of DCFC with molten hydroxide electrolyte.

## 2 Experimental study of direct carbon fuel cell

### 2.1 Electrolyte and fuel

The binary eutectic mixture (90–10 mol%) of alkaline earth metal hydroxides NaOH and LiOH (supplied by POCH corp.) was selected for the investigations. The fuel used for the investigation was biochar derived from the carbonization of apple tree chips (particle size  $< 0.5 \times 10^{-3}$  m) at 873 K for 30 min. Biochar was analyzed according to Polish standards with respect to their ultimate and proximate analysis. The ultimate analysis was conducted with the use of Leco TruSpec CHNS analyzer [5,6], while automatic isoperibol calorimeter (IKA C2000 Basic [7]) was used to determine the higher

heating values (HHV) of all the samples. Mercury intrusion porosimeter (Poremaster 33, Quantachrome [8]) was used to determine the total surface areas and pore volumes of the samples, as well as to investigate the pore size distributions. The results of the analyses are summarized in Tab. 1.

Table 1. Main parameters of the fuels tested (all values are given for a ‘dry’ state).

Fuel sample	Ultimate analysis [wt%]					Ash [wt%]	Volatile matter [wt%]	Higher heating value [MJ kg <sup>-1</sup> ]	Surface area [m <sup>2</sup> kg <sup>-1</sup> ]	Pore volume [m <sup>3</sup> kg <sup>-1</sup> ]
	C	H	N	S	O <sup>dfff</sup>					
Biochar	80.3	2.8	1.9	0.00	4.30	10.7	16.8	29.55	6650	0.25 × 10 <sup>-3</sup>

## 2.2 DCFC test setup

The experiments were conducted in a laboratory-scale DCFC test cell shown schematically in Fig. 1.

The cell was manufactured from nickel and nickel alloys. The anode and cathode chambers were separated in order to prevent any mixing at the gases (CO<sub>2</sub> above the anode and excess air above the cathode). The main cell was manufactured from Nickel 201. The anode was also made from Nickel 201, while the cathode was Ni-based Inconel alloy 600. The details of configuration and the operating mechanism of DCFC cell was described elsewhere [9,10].

## 2.3 Fuel cell performance test methodology

The experiments described in the present paper were conducted in a laboratory-scale facility shown in Fig. 2. The electrolyte temperature was determined by a K-type thermocouple (NiCr-NiAl) and was maintained at the desired value by an electronic temperature controller. The data acquisition module Advantech USB-4711A [11] was used for the measurement of the cell voltage and the decrease of the voltage on an external resistor. In order to determine the cell current and power at various loads an external resistance setup MDR-93/2-52 [12] was used and connected to the cell circuit thus providing the possibility to adjust the electrical resistance of the external circuit (in range 0.1–10.000 Ω). The Tektronix DMM 4040 digital multimeter [13] was used to measure the open circuit voltage of the fuel cell. The

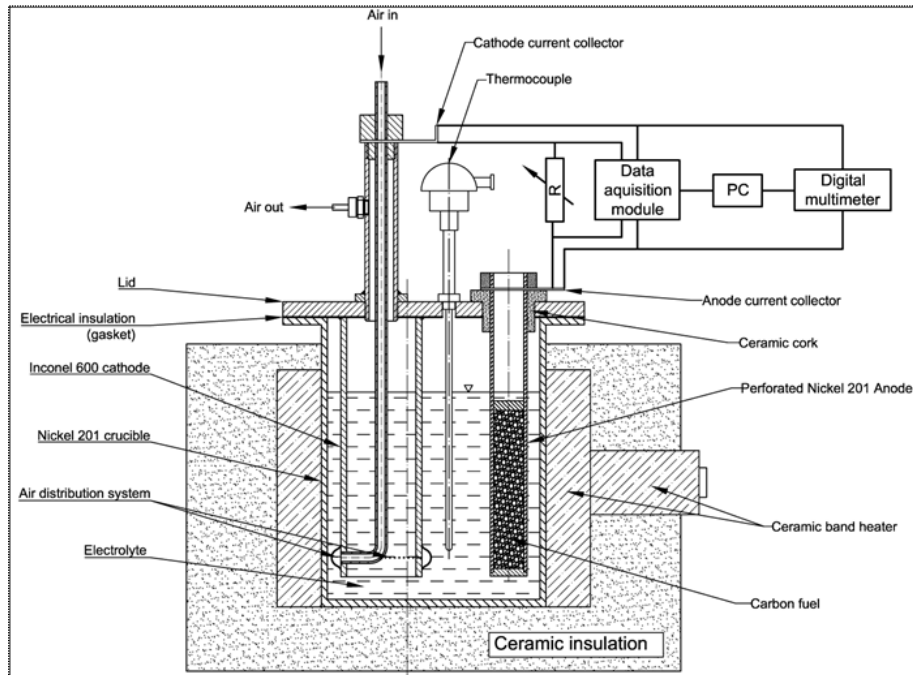


Figure 1. The outline of the experimental DCFC setup.



Figure 2. The picture of the laboratory-scale testing facility for DCFC.

acquisition module and multimeter were connected to a personal computer (PC) where the data was displayed and stored. The amount of air fed into the cell was controlled by a thermal mass flow controller (Brooks 4850) [14] with local operator interface (LOI) to view, control and configure the control device. It was possible to adjust the gas flow rate from  $1.7 \times 10^{-6} \text{ m}^3\text{s}^{-1}$  to  $33.3 \times 10^{-6} \text{ m}^3\text{s}^{-1}$ . In order to attenuate short-term surge suppression

and eliminate the effects of power grid interferences on the recorded data, the emergency standby backup power device PowerCom UPS BNT-1500AP with the noise filter EMI/RFI [15], was also used during the experiments.

At the beginning of each test eutectic mixture of NaOH (90 mol%) with LiOH (10 mol%) was prepared and then heated up to the desired temperature. After the temperature level of 723 K was reached and the electrolyte was completely molten, both the cathode and the anode were slowly immersed into the electrolyte and the cell data (current intensity, voltage, temperature, etc.) were recorded. After each test was finished the heating was turned off and the cell was 'shutdown'. The setup was then cooled down to room temperature and then all its parts were placed in special plastic container filled with roughly 0.025 m<sup>3</sup> of deionized water. All the elements were kept there for three hours in order to get the solidified electrolyte removed. A mechanical stirrer was used to improve the dissolution of the electrolyte. The water-electrolyte mixture was then removed and a new portion of 0.025 m<sup>3</sup> of deionized water was put into the container. The whole procedure was then repeated. Afterwards, the cell elements were removed from the container, cleaned with a soft sponge, and finally again rinsed with deionized water. All the elements were then dried for 3 h in a drier.

## 3 Results and discussion

### 3.1 The effect of electrolyte temperature

Figure 3 shows curves of cell potential and output power density versus current density at different temperatures of the electrolyte. The air flow rate in this study was maintained at  $8.3 \times 10^{-6} \text{ m}^3\text{s}^{-1}$ . The main electrical parameters obtained from the study are summarized in Tab. 2. The results indicate that the increase of the temperature brings about increases of the electrical parameters of the cell. The current and power densities achieved at temperature of 773 K were twice as high as the results obtained at 673 K. One of the reasons that the fuel cell generated higher power density and current was probably the improved conductivity of electrolyte, in addition to the increased reaction rate. The increased temperature not only improves the performance of the cell, but also has an impact on the corrosion processes that may lead to the subsequent shutdown of fuel cell. Only long-term corrosion tests of cell operating at higher temperatures can determine the impact of increased temperature on the created oxide layers

that determine reliable and continuous operation of the fuel cell.

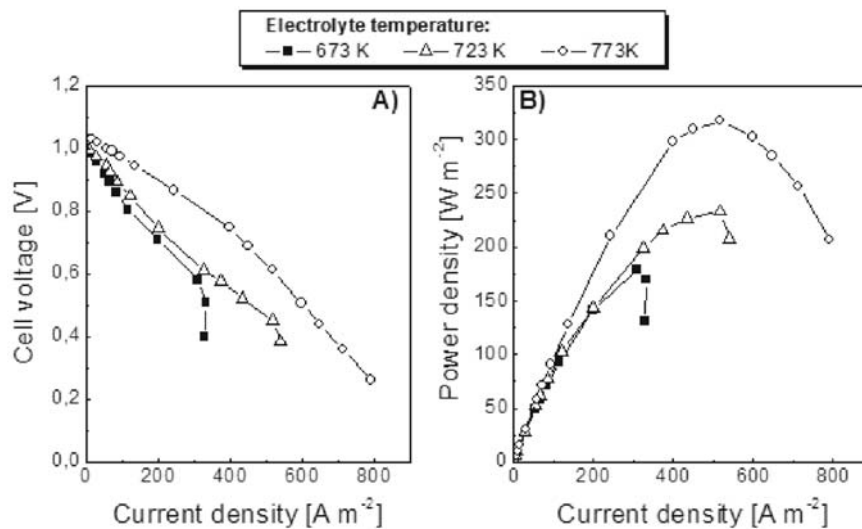


Figure 3. Cell voltage vs. current density (A) and power density vs. current density (B) curves for different electrolyte temperatures (fuel: biochar, air flow rate:  $8.3 \times 10^{-6} \text{ m}^3 \text{ s}^{-1}$ , particle size:  $0.18 \times 10^{-3} - 0.25 \times 10^{-3} \text{ m}$ ).

Table 2. Summary of the operational parameters for the operation of the DCFC (various electrolyte temperatures, air flow rate:  $8.3 \times 10^{-6} \text{ m}^3 \text{ s}^{-1}$ , fuel: biochar, particle size:  $0.18 \times 10^{-3} - 0.25 \times 10^{-3} \text{ m}$ ).

Electrolyte temperature [K]	Electromotive force [V]	Max. power density [W m <sup>-2</sup> ]	Current density at 0.5 V [A m <sup>-2</sup> ]
673	$0.9985 \pm 0.0003$	179	333
723	$1.0008 \pm 0.0005$	224	446
773	$1.0402 \pm 0.0008$	318	601

### 3.2 The effect of air flow rate

The polarization and power characteristics of the cell operated with various cathode inlet air flow rates are shown in Fig. 4. The main operation parameters of the fuel cell are summarized in Tab. 3. Both data indicate

that both too small and too large air flow rates to the cathode chamber of fuel cell had a negative influence on DCFC electrical parameters. For air flow rate of  $0.5 \times 10^{-6} \text{ m}^3\text{s}^{-1}$  the fuel cell achieved the lowest current density, while for the  $8.3 \times 10^{-6} \text{ m}^3\text{s}^{-1}$  the best results were achieved for both current and power density. Characteristic curves are similar to those obtained by Hackett [16], who observed that increasing the amount of supply air results in a decrease in current and power densities. Analysis of the shapes of characteristic curves shows that the low value of the air flow rate affects the deterioration of the cell performance. This may be related to insufficient amount of substrate ( $\text{O}_2$ ) in the reduction reaction which occurs on the cathode surface. The higher reaction rate, related to higher current generated by fuel cell results in increased demand for the oxygen which is contained in the air fed to the cathode. On the other hand, too high a value of air flow ( $13.3 \times 10^{-6} \text{ m}^3\text{s}^{-1}$ ) makes a lot of gas bubbles, which are formed at the surface of the electrode, limited the reaction surface area and thus the fuel cell achieves worse electrical parameters. The results of the research indicate that fuel cell operates best for average values of air flow rates — from  $3.3 \times 10^{-6}$  to  $8.3 \times 10^{-6} \text{ m}^3\text{s}^{-1}$ . Most preferred amount of air supplied to the tested model was  $8.3 \times 10^{-6} \text{ m}^3\text{s}^{-1}$ .

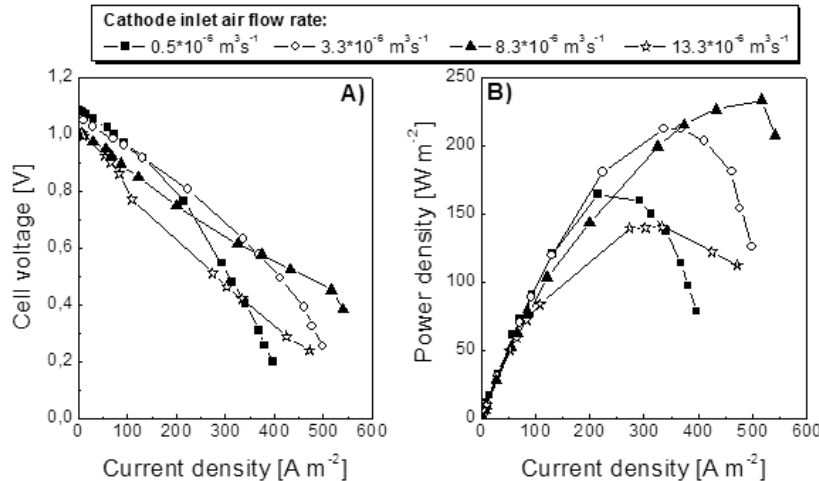


Figure 4. Cell voltage vs. current density (A) and power density vs. current density (B) curves for different cathode inlet air flow rates (fuel: biochar, particle size:  $0.18 \times 10^{-3} - 0.25 \times 10^{-3} \text{ m}$ , electrolyte temperature: 723 K).

Table 3. Summary of the operational parameters for the operation of the DCFC (various air flow rates, electrolyte temperature: 723 K, particle size:  $0.18 \times 10^{-3} - 0.25 \times 10^{-3}$  m, fuel: biochar).

Air flow rate [ $\text{m}^3\text{s}^{-1}$ ]	Electromotive force [V]	Max. power density [ $\text{W m}^{-2}$ ]	Current density at 0.5 V [ $\text{A m}^{-2}$ ]
$0.5 \times 10^{-6}$	$1.0830 \pm 0.0011$	164	309
$3.3 \times 10^{-6}$	$1.0541 \pm 0.0029$	212	407
$8.3 \times 10^{-6}$	$1.0008 \pm 0.0005$	224	446
$13.3 \times 10^{-6}$	$1.0087 \pm 0.0004$	140	279

### 3.3 The effect of fuel particles size

In Fig. 5 the characteristics of the DCFC operated with various fuel particles size are shown while the main electrical parameters are summarized in Tab. 4. These results indicate that the size of biochar particles directly

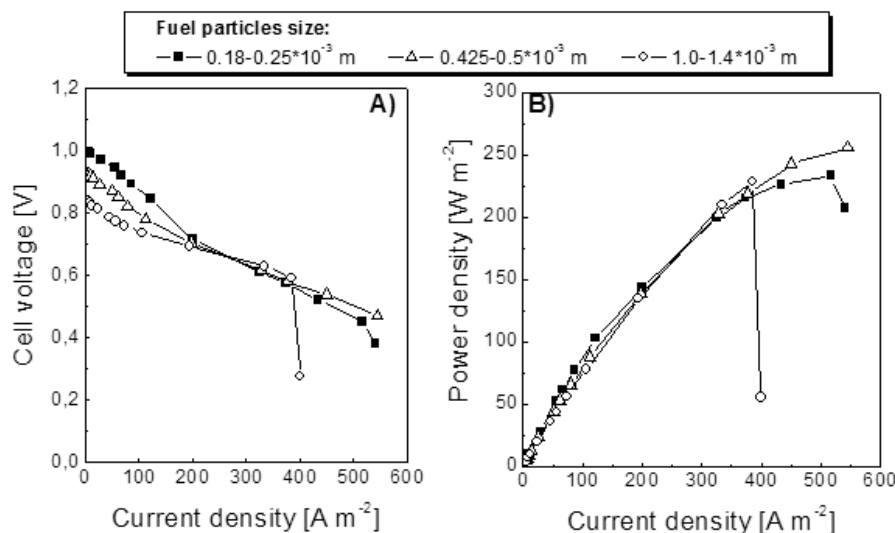


Figure 5. Cell voltage vs. current density (A) and power density vs. current density (B) curves for different fuel particles size (fuel: biochar, air flow rate:  $8.3 \times 10^{-6} \text{m}^3\text{s}^{-1}$ , electrolyte temperature: 723 K).

affects the value of the electromotive force. Generally, the larger the fuel particle size the lower the cell voltage. The worst results were obtained



for biochar with particle size range of  $1 \times 10^{-3} - 1.4 \times 10^{-3}$  m, while the highest density was obtained for fuel particle size range of  $0.425 \times 10^{-3} - 0.5 \times 10^{-3}$  m. Better performance of fuel cell fed by a fuel with a medium particle size ( $0.425 \times 10^{-3} - 0.5 \times 10^{-3}$  m) compared to the performance of cell which was fed by a fuel with a smaller particle size ( $0.18 \times 10^{-3} - 0.25 \times 10^{-3}$  m) may suggest that larger spaces between the biochar grains positively affect the cell operation. However, the results of the analysis of the voltage-current characteristics indicate that the principle has failed for larger fuel particles. Therefore it can be concluded that apart from a larger intergranular space available for electrolyte the contact surface between fuel grains and anode current collector is also important, as observed in the case of biochar with particle sizes of  $0.425 \times 10^{-3} - 0.5 \times 10^{-3}$  m.

Table 4. Summary of the operational parameters for the operation of the DCFE (various particles size, air flow rate:  $8.3 \times 10^{-6} \text{ m}^3 \text{ s}^{-1}$ , electrolyte temperature: 723 K, fuel: biochar).

Particle size [m]	Electromotive force [V]	Max. power density [W m <sup>-2</sup> ]	Current density at 0.5 V [A m <sup>-2</sup> ]
$0.18 \times 10^{-3} - 0.25 \times 10^{-3}$	$1.0008 \pm 0.0005$	224	446
$0.425 \times 10^{-3} - 0.5 \times 10^{-3}$	$0.9292 \pm 0.0039$	256	503
$1 \times 10^{-3} - 1.4 \times 10^{-3}$	$0.8245 \pm 0.0043$	228	389

## 4 Conclusions

On the basis of the analysis of the information discussed in the present paper the following major conclusions may be formulated:

1. The increase of the electrolyte temperature brings about increase of the current and power densities — the power and current densities obtained at 773 K were twice as high as those at 673 K.
2. Both too small and too large air flow rates negatively affect the cell performance. The best cell performance was achieved for the air flow rate of  $8.3 \times 10^{-6} \text{ m}^3 \text{ s}^{-1}$ .
3. The size of biochar particles affects the cell voltage. Generally, the larger the particle size the lower output voltage. The best results were

obtained for biochar particle sizes of  $0.18 \times 10^{-3} - 0.25 \times 10^{-3}$  m, and  $0.425 \times 10^{-3} - 0.5 \times 10^{-3}$  m, while the worst results were determined for biochars of roughly  $1 \times 10^{-3} - 1.4 \times 10^{-3}$  m.

**Acknowledgment** This work has been supported by the Polish Ministry of Education and Science under grant No. N N513 396 736. One of the authors (A. Kacprzak) is also indebted for the financial support to the DoktoRIS - Scholarship Program for Innovative Silesia, co-financed by the European Union within the framework of the European Social Fund.

*Received 14 October 2013*

## References

- [1] CAO D., SUN Y., WANG G.: *Direct carbon fuel cell: Fundamentals and recent developments*. J Power Sources **167**(2007), 250–257.
- [2] COOPER J.F.: *Direct conversion of coal derived carbon in fuel cells*. In: Recent Trends in Fuel Cell Science and Technology, Chap. 10 (S. Basu, Ed.), Springer and Anamaya, 2007, 248–266.
- [3] GIDDEY S., BADWAL S.P.S., KULKARNI A., MUNNINGS C.: *A comprehensive review of direct carbon fuel cell technology*. Prog. Energy Combust. Sci. **38**(2012), 360–399.
- [4] ZECEVIC S., PATTON E.M., PARHAMI P.: *Direct electrochemical power generation from carbon in fuel cells with molten hydroxide electrolyte*. Chem. Eng. Commun. **192**(2005), 1655–1670.
- [5] PN-EN 15104:2011E – Solid biofuels... (in Polish).
- [6] PN-G-04584:2001P – Solid fuels... (in Polish).
- [7] PN-C-04375-2:2013-07P – Investigations of solid and liquid fuels... (in Polish).
- [8] DIN 66133 – Determination of pore volume distribution and specific surface area of solids by mercury intrusion.
- [9] KACPRZAK A., KOBYLECKI R., BIS Z.: *Influence of temperature and composition of NaOH-KOH and NaOH-LiOH electrolytes on the performance of a direct carbon fuel cell*. J. Power Sources **239**(2013), 409–414.
- [10] KACPRZAK A., WŁODARCZYK R., KOBYLECKI R., ŚCISŁOWSKA M., BIS Z.: *Fuel cell as part of clean technologies*. In: Environmental Engineering IV, (Pawłowski A., Dudzińska M.R., Pawłowski L., Eds.), CRC Press, Taylor & Francis Group, London 2013, 443–450, ISBN 978-0-415-64338-2.
- [11] Advantech USB-4711A datasheet: [http://downloadt.advantech.com/ProductFile/PIS/USB-4711A/Product%20-%20Datashet/USB-4711A\\_DS20130703153611.pdf](http://downloadt.advantech.com/ProductFile/PIS/USB-4711A/Product%20-%20Datashet/USB-4711A_DS20130703153611.pdf).
- [12] Resistance setup type MDR-93/2-5a datasheet: [http://www.kompartpomiar.pl/pobierz.php?plik=dok\\_mdr.pdf&u=dt](http://www.kompartpomiar.pl/pobierz.php?plik=dok_mdr.pdf&u=dt).

- 
- [13] Tektronix DMM 4040 digital multimeter datasheet: <http://www.tek.com/sites/tek.com/files/media/media/resources/Tektronix-DMM4050-and-DMM4040-Digital-Multimeter-Datasheet-8.pdf>
  - [14] Mass flow controller Brooks 4850 datasheet: <http://www.brooksinstrument.com/downloads/Product%20Documentation/Thermal%20Mass%20Flow%20Meters%20Controllers%20Digital%20Gas/Data%20Sheets/ds-tmf-4800-mfc-eng.pdf>.
  - [15] Backup power device Powercom BNT 1500AP datasheet: <http://www.powercom-usa.com/ProductDetail.asp?ID=3978>
  - [16] HACKETT G. A., ZONDLO J. W., SVENSSON R.: *Evaluation of carbon materials for use in a direct carbon fuel cell*. J. Power Sources **168**(2007), 111–118.